

# Molecular dynamics simulation of diffusion and permeation of gases in polystyrene

Farkhondeh Mozaffari<sup>a,\*</sup>, Hossein Eslami<sup>b,c</sup>, Jalil Moghadasi<sup>a</sup>

<sup>a</sup>Department of Chemistry, College of Sciences, Shiraz University, Shiraz 71454, Iran

<sup>b</sup>Department of Chemistry, College of Sciences, Persian Gulf University, Boushehr 75168, Iran

<sup>c</sup>Eduard-Zintl Institut für Anorganische und Physikalische Chemie, Technische Universität Darmstadt, Petersenstraße 20, D-64287, Germany

## ARTICLE INFO

### Article history:

Received 14 July 2009

Received in revised form

19 October 2009

Accepted 21 October 2009

Available online 10 November 2009

### Keywords:

Diffusion coefficient

Molecular dynamics simulations

Permeation

## ABSTRACT

Molecular dynamics simulations are performed to study the diffusion and permeation of gases, including argon, nitrogen, methane, carbon dioxide, and propane, in polystyrene over a wide range of temperatures. A jumping mechanism is observed for the diffusion of diffusants in polymer. The calculated diffusion coefficients agree well with the experimental data and with the results of former simulation studies. The relation between the diffusion coefficient and the molecular diameter is confirmed by the results. Our calculated results on the temperature-dependence of diffusion coefficients show that for some gases a break is seen, at the glass transition temperature, in the Arrhenius plot of  $\ln(D)$  versus  $1/T$ , while for some other light gases, argon and nitrogen, the plot is linear over the whole temperature range. We have also calculated the permeability coefficients, using the diffusion coefficients calculated in this work and our recently published solubility coefficients [Eslami and Müller-Plathe, *Macromolecules* 2007; 40:6413]. Our results show that the calculated permeability coefficients are higher than the experimental data by almost the same trend observed in the solubility calculations, but the ratios of calculated permeabilities are in a very good agreement with experiment.

© 2009 Elsevier Ltd. All rights reserved.

## 1. Introduction

The development of more efficient methods of separating fluid mixtures, which has always been of great interest to the chemical industry, has been further spurred by the energy crisis of recent years. One of the promising separation techniques, being studied in many academic and industrial laboratories, is based on the selective permeation or transport of fluids through nonporous polymer membranes. Therefore, the knowledge of the diffusion coefficient of gases in polymers is very important in many industrial processes such as separation of gases by selective permeation through polymer membranes, food packaging, protective coatings, biomedical devices (e.g., the heart lung machine). Drug delivery systems are largely based on the advances in polymer chemistry, e.g., the ability to fabricate different polymeric materials for controlling the diffusion of drug molecules. Release of drug molecules at a certain desirable rate are controlled by polymeric membranes or materials.

Most theories describing the mechanism of diffusion in polymeric materials are based on the free volume approximation [1–3]. In the free volume theories, there is a volume which is directly occupied by polymeric molecules, and there is the remainder of the volume,

which is called the free volume. A part of the free volume is assumed to be uniformly distributed among the molecules and is identified as the interstitial free volume, which requires a large energy for redistribution and is not affected by random thermal fluctuations. The other part, which is called the hole free volume, is assumed to require negligible energy for its redistribution. Therefore, the hole free volume is being continuously redistributed due to random fluctuations, and is assumed to be occupied by penetrant molecules. This redistribution of hole free volume will move the penetrant molecule with it. According to this model, by movement of segments of the polymer chain, a void will be created adjacent to the penetrant molecule. If the size of this hole is sufficient to host a penetrant molecule and if the penetrant have sufficient energy to jump into the hole, a successful jump of the penetrant molecule is made into the hole. Although the free volume model has been used extensively to describe the mechanism of transport through molten or glassy polymers [4–7], this model does not show a microscopic view point of penetrant transport in polymers, since it just connects bulk transport properties, like diffusion coefficient, into bulk properties, like molecular volume or thermal expansion coefficient.

The transition-state theory (TST), introduced by Arizzi [8] and by Gusev et al. [9,10], is another useful method for the calculation of diffusion coefficient of a low-molar-mass substance through the polymer matrix. In the TST it is assumed that the movement of the

\* Corresponding author. Tel.: +98 9173027645.

E-mail address: [mozaffarif@yahoo.com](mailto:mozaffarif@yahoo.com) (F. Mozaffari).

penetrant from an initial cavity to the saddle point and to a neighboring cavity is an unimolecular rearrangement. For such a transition the reaction trajectory in configuration space is tracked and the transition rate constant is evaluated. In the first studies on the application of TST to study the dynamics of light gases dissolved in rigid microstructures of glassy polycarbonate and rubbery polyisobutylene [9], the method was shown to be only capable to study just the dynamics of light gas like He. The method was developed by Gusev and Suter [10], by Gusev et al. [11], and by Theodorou et al. [12–15], to calculate the diffusion coefficient of bigger penetrants in glassy polymers.

Computer modeling of molecular systems at a detailed atomistic level has become a standard tool in investigation of sorption and diffusion of small molecules in polymeric media [11,16–19]. Molecular dynamics simulation is a useful tool for exploring the structure and properties of bulk amorphous polymers. The length of the trajectories that can be generated in practice presently is on the order of many nanoseconds. Thus the range of properties that can be studied directly is limited to those that evolve over this time scale. One of the phenomena that appear to be suitable for investigation is the diffusion of small penetrant molecules in an amorphous polymeric matrix. That is, the diffusion coefficients of small penetrants in many rubbery or liquid polymers are such that, at temperatures close to room temperature and above, the average displacement of the diffusant is large enough in a nanosecond interval to be determined *via* molecular dynamics simulation. Performing such simulations is of practical importance in predicting diffusion coefficients and also in understanding the mechanism of diffusion.

Although there has been significant progress in the use of molecular dynamics methods in the simulations of diffusion coefficients, early studies were focused on the simulation of gas diffusion in rubbery polymers which could be investigated using full atomistic or united-atom simulations in reasonable computational times [20–25]. Due to the recent development of improved force fields and the wider availability of sophisticated commercial softwares and high-speed computing facilities, attention is shifting to direct to the more challenging task of simulating the slower diffusional processes occurring in glassy polymers [19,26–31]. In most of the computational studies on the sorption and diffusion of penetrants in polymers, the authors have dealt with flexible polymer chains of relatively simple structure such as polyethylene, polypropylene, and poly(isobutylene) [16,17,24,32–36]. There are, however, some reports on polymers consisting of stiff chains. As some examples we may address to the works by Mooney and MacElroy [37] on the diffusion of small molecules in semicrystalline aromatic polymers, by Cuthbert et al. [38] on the calculation of Henry's law constant for a number of small molecules in polystyrene and studying the effect of box size on the calculated Henry's law constants, by Lim et al. [31] on the sorption and diffusion of methane and carbon dioxide in amorphous poly(ether imide), and by Milano et al. [19] on the calculation of anisotropic diffusion of helium and carbon dioxide in crystalline syndiotactic polystyrene.

Very recently we have performed extensive molecular dynamics simulation studies of sorption of penetrant molecules in polystyrene over a wide range of temperatures, 300 K–500 K [39]. To this end, we have developed a method for the calculation of the solubilities of penetrants in polymers [40]. It is the purpose of this work to calculate the diffusion coefficient of the same penetrant gases in polystyrene, over the same temperature range, which is useful for the calculation of permeability coefficient of penetrants in polystyrene.

## 2. Theory

One of the straightforward ways of studying the motion of individual atoms or molecules is molecular dynamics. The molecular

dynamics method tracks the time evolution, at the atomic level, of an ensemble of particles acting under specified interatomic forces by numerically solving the equations of motion in an iterative manner. In order to calculate the diffusion coefficients by molecular dynamics simulation, one has to calculate the center-of-mass mean-square displacements. In the limit of long times, which the penetrant molecules perform random walks in the polymer matrix, the mean-square-displacement becomes linear in time, and the diffusion coefficients can be calculated using the Einstein relation:

$$D = \frac{1}{6N} \lim_{t \rightarrow \infty} \frac{d}{dt} \left\langle \sum_i^N [\mathbf{r}_i(t) - \mathbf{r}_i(0)]^2 \right\rangle \quad (1)$$

where  $D$  is the diffusion coefficient,  $\mathbf{r}_i$  is the center-of-mass position vector of penetrant  $i$ ,  $N$  is the total number of penetrants,  $t$  is the time, and the brackets represent averaging over all possible time origins.

For diffusion of penetrants in polymers, the center-of-mass mean-square-displacement of the penetrant is shown to pass through three distinct regimes [11]. The first is the short-time ballistic regime. Then a regime of anomalous diffusion occurs, in which the mean-square-displacement is proportional to  $t^\alpha$  with  $\alpha < 1$ . Finally, for sufficiently long times, the Fickian regime occurs, for which the mean-square-displacement is proportional to  $t$ , Eq. (1). The reason for anomalous diffusion is a structure of the environment which alters the possible diffusion pathway by introducing extra tortuosity on a certain length scale, or which delays the diffusion by forcing the diffusants to adopt certain shapes in order to be able to slip through openings [41,42].

The solubility of permeant molecule in the membrane is the second determining factor in the permeation process. The solubility-diffusion mechanism postulates that permeation is controlled by diffusion of the permeant gas in the membrane which is assumed to be in thermodynamic equilibrium with the gas at the interfaces. Thus, the permeability coefficient,  $Pe$ , is defined by the ratio between the flux  $J$  of the permeant species and its concentration gradient,  $\Delta c$ , over the membrane of thickness,  $d$ , i.e.,

$$J = Pe \frac{\Delta c}{d} \quad (2)$$

The permeability coefficient is given by the product of the diffusion coefficient,  $D$ , and the solubility coefficient,  $S$ , as:

$$Pe = DS \quad (3)$$

The permeability is then the product of a factor reflecting the dynamics of the penetrant-polymer system,  $D$ , and a thermodynamic factor depending on the penetrant-polymer interactions,  $S$ . Therefore, the permeability shows the ease with which the gas crosses the polymer film.

Independent determinations of  $D$  and  $S$  are possible from atomistic simulations [11,19–24,32,33,43–46], such that the influence of chemical architecture and polymer morphology on the over all permeability can be examined in detail. Atomistic simulations not only provide a method for estimating both  $D$  and  $S$ , but also offer insight into the molecular mechanisms of penetrant transport through the polymer. The ability to calculate changes in permeability resulting from modifications of the chemical and structural properties of polymer membranes suggests a direct application of atomistic simulations to improve membrane performance and ultimately to design new membranes from first principles.

In this study, molecular dynamics simulation technique has been applied to calculate the diffusion coefficient of some penetrant gases including argon, nitrogen, carbon dioxide, methane, and propane in polystyrene over a wide range of temperatures. Using

the solubility coefficients of these gases, from the results of our former molecular dynamics simulation study [39], we have calculated the permeability coefficients as well.

### 3. Simulation

Simulations were performed for mixtures of polystyrene plus the penetrant gases argon, nitrogen, carbon dioxide, methane, and propane over a wide range of temperatures, at zero penetrant pressure limit (the number of molecules is calculated based on the solubility of gases in polystyrene [39]). The potential energy parameters for polystyrene were reported previously [47]. Here, it is just sufficient to say that parameters for aliphatic carbon and hydrogen are those used before for polyolefins [48], and the phenyl groups of polystyrene were described by the same parameters as the benzene model of Jorgensen and Severance [49]. The barrier height for rotation of polystyrene backbone dihedral angles was adopted as  $12 \text{ kJ mol}^{-1}$ , following the ab initio calculations on polystyrene fragments [47]. The parameters for unlike interactions were determined using the Lorentz–Berthelot mixing rules [50]. The force field has been checked against the experimental pressure–volume–temperature data of polystyrene [47]. An atactic random polystyrene chain of 100 monomers, generated [47] in vacuum using the rotational isometric state theory with the weights of Rapold [51], was used. The details of the molecular dynamics simulation are reported in our former publication on the solubility of the afore-cited penetrant gases in polystyrene [39]. It is sufficient to say that coupling of the system to temperature bath and barostat was performed using Berendsen's method [52], with coupling times of 0.2 ps for coupling to the thermostat and 5.0 ps for coupling to the barostat. The time-step for leapfrog integration scheme was 1.5 fs and all bond lengths were constrained using the SHAKE algorithm [53,54]. The cutoff distance was 1.0 nm, and the reaction field correction for the Coulombic interactions [55] was included, with the effective dielectric constant of 2.5. An atomic Verlet neighbor list was used, which was updated every 15 time-steps, and the neighbors were included if they were closer than 1.1 nm. Similar to the former work [39], all equilibrium configurations of the model polymer at lower temperatures were produced by cooling the system down with a temperature step of 20 K for around 3 ns. The glass transition temperature of polystyrene, as is reported in our former study [39], is 370 K. The Lennard–Jones potential parameters used to calculate the interaction energy for penetrant gases and the host polymer, are those reported in our former work [39].

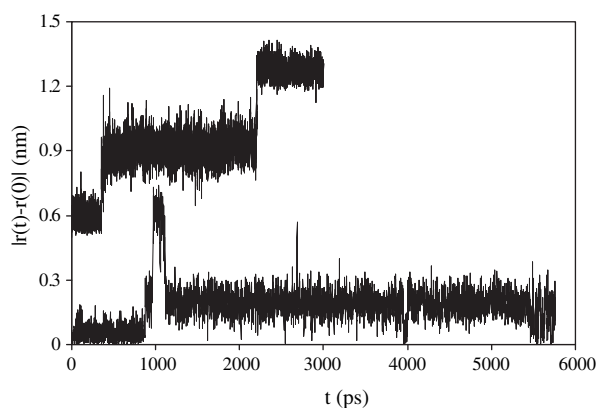


Fig. 1. Displacement of argon and propane molecules from their initial positions at 300 K. In order to avoid overlapping between the curves, the displacements of argon are offset by 0.6 nm.

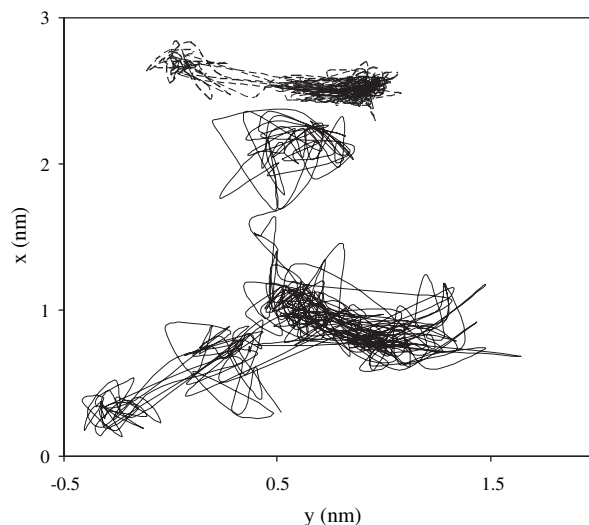


Fig. 2. Typical trajectories of nitrogen molecules in polystyrene at 300 K (upper curve) and 500 K (lower curve).

## 4. Results and discussions

### 4.1. Penetrant center-of-mass displacements

The motion pattern of penetrant gases in host polymer can be qualitatively studied by monitoring the penetrant's displacement  $|r(t)-r(0)|$ , from its initial position. Shown in Fig. 1 are the displacements of argon and propane in polystyrene at 300 K. The curves are representative of a common hopping mechanism, showing that for a considerable time interval the penetrants dwell in existing voids in the polymer and occasionally do a jump into the neighboring voids. When dwelling in the voids, the penetrants just perform oscillatory motions around their equilibrium positions, therefore, no net motion of a penetrant molecule occurs with these positional fluctuations. The amplitude of oscillations varies according to the size of voids. From time to time, the penetrants can do a quick jump into their neighboring voids, see Fig. 1. The jump frequency depends on penetrant's size, therefore the biggest penetrant studied in this work, propane, can rarely jump between the voids.

The two-dimensional center-of-mass  $x$ - $y$  trajectories of nitrogen in polystyrene at temperatures below and above the glass transition temperature, 300 K and 500 K, respectively, are shown in Fig. 2. The penetrant trajectories indicate faster movement of

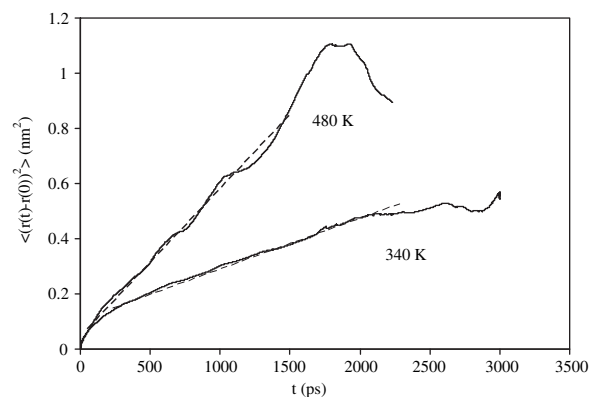


Fig. 3. Center-of-mass mean-square displacement for carbon dioxide at temperatures below and higher than the glass transition temperature. The curve at 480 K is scaled down by a factor of 15 for the sake of clarity. The dashed lines show the least-squares fits to the curves.

penetrants at higher temperatures, as represented by the broadened range of displacements at higher temperatures in Fig. 2. This indicates that at higher temperatures the hole free volume will be redistributed faster and penetrant molecules have higher energy to overcome the activation energy required to jump into new voids.

#### 4.2. Penetrant center-of-mass mean-square displacements

The mean-square displacement of penetrant gases are calculated over a wide range of temperatures, 300 K–500 K, in 20 K intervals. Averaging is performed over all penetrant molecules and all possible time origins. This leads to an increase of statistical fluctuations towards the end of the run. The results for the center-of-mass mean-square displacements of carbon dioxide at temperatures below and above the glass transition temperature, 340 K and 480 K, respectively, and those of argon, methane, and propane at 440 K are shown in Figs. 3 and 4, respectively. Log–log plots (not shown) of the center-of-mass mean-square displacement versus time for carbon dioxide at 340 K and 480 K fit quite well with straight lines with slopes 0.97 and 1.04, respectively, confirming the Einstein diffusion. In the glassy polymer at times below 500 ps, the penetrant motion is highly anomalous and the diffusion regime begins at longer times. Intercavity jumps rarely occur at this time scale [19,56]. However, as it can be seen from the results in Fig. 3 at high temperatures, the diffusion regime sets in a shorter time. Also the results in Fig. 4 for center-of-mass mean-square displacement of argon, methane, and propane, show that the mean-square displacements of the smaller penetrant molecules are much closer to linearity than those of bigger molecules. In fact for bigger molecules like propane, there are much fewer jumps than there are for a smaller molecule. Therefore the statistical error is bigger in the former case.

The linear portion of the center-of-mass mean-square displacement is least-squares fitted by a straight line to calculate the diffusion coefficient. The calculated diffusion coefficients at 300 K are tabulated in Table 1 and are compared with experimental data [57–60] and with the results of former simulation studies in the literature [28,61]. The results are almost in good agreement with experimental data [57–60] and with the results of former simulation studies, reported in the literature [28,61]. The only exception is the big

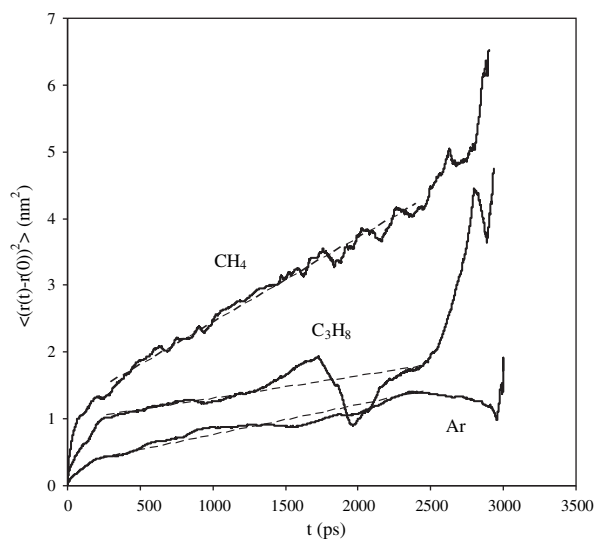


**Fig. 4.** Center-of-mass mean-square displacement for argon, methane, and propane at 440 K. The curve for argon is scaled down by a factor of 2 and that for propane is scaled up by a factor of 15, to make the details more visible. The dashed lines show the least-squares fits to the curves.

**Table 1**

Comparison of the calculated diffusion coefficients of penetrant gases at 300 K with experimental data [57–60] and with the results of former simulation works [28,61].

Penetrant	$D_{\text{exp.}} \times 10^8 \text{ (cm}^2 \text{ s}^{-1}\text{)}$	$D_{\text{cal.}} \times 10^8 \text{ (cm}^2 \text{ s}^{-1}\text{)}$	
		Previous simulations	This work
Ar	7.0 <sup>a</sup>	2.0, 7.30 <sup>e</sup>	7.50
N <sub>2</sub>	6.0 <sup>b</sup>	6.10 <sup>e</sup>	6.20
CO <sub>2</sub>	5.08 <sup>c</sup>	3.30 <sup>e</sup>	6.44
CH <sub>4</sub>	1.30 <sup>d</sup>	1.20 <sup>e</sup> , 1.60 <sup>f</sup>	1.50
C <sub>3</sub> H <sub>8</sub>	0.002 <sup>d</sup>		0.0042

<sup>a</sup> Ref. [57].

<sup>b</sup> Ref. [58].

<sup>c</sup> Ref. [59].

<sup>d</sup> Ref. [60].

<sup>e</sup> Ref. [61].

<sup>f</sup> Ref. [28].

molecule propane, for which our calculated value for the diffusion coefficient at 300 K is bigger than the experimental value [60] by a factor of 2. A simple estimation of  $D$  based on  $D = d^2/6\tau$ , which  $d$  is the jump distance, about 0.5 nm (see Fig. 1), and  $\tau$  is the cavity residence time, gives  $\tau \approx 100$  ns. This means that propane resides in its cavity for about 100 ns, on average, before jumping to another cavity. To have a sufficient statistics to calculate the diffusion coefficient one needs about 10 jumps, and hence, simulation times of the order of  $\mu\text{s}$  are required. Therefore, the calculated diffusion coefficient for propane in this work can just qualitatively be compared with experiment [60].

There are many correlation schemes trying to connect the diffusion coefficients of penetrant gases in polymers to the structural properties of the penetrant gas [61–64]. Almost all of these procedures are based on the empirical approaches and are restricted to a single host polymer, but are valid for a variety of penetrants. The nature and the size of the penetrant gas molecules which cross the membrane are parameters affecting the diffusion coefficient of the penetrant molecules in polymers. These characteristics are taken into account by means of the Lennard–Jones parameters of the gas molecule, namely, the effective diameter, and the characteristic interaction energy between molecules. Although numerous attempts were made [65], it is impossible to find a model of general validity describing the dependence of diffusion coefficients on these parameters.

Based on extensive experimental data with different penetrants and polymer hosts, Teplyakov and Meares [66] have developed the

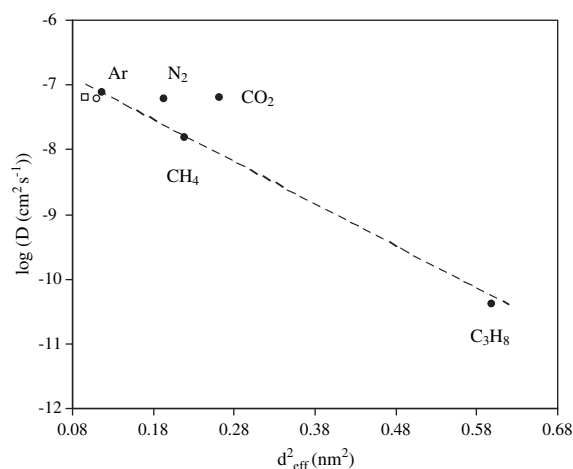


**Fig. 5.** Logarithm of the diffusion coefficients as a function of square effective diameters. The open circle and open square show the results for nitrogen and carbon dioxide when the Lennard–Jones  $\sigma$  of one interaction site is adopted as the effective diameter.

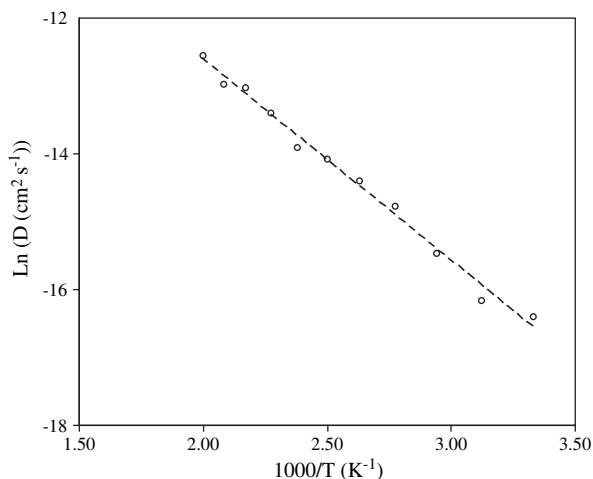


Fig. 6. Arrhenius plot of  $\ln(D)$  versus  $1/T$  for argon. The dashed line indicates the best fit through the points.

following correlation between the diffusion coefficient of penetrant gases and their effective diameters.

$$\ln(D) = K_1 - K_2 d_{\text{eff}}^2 \quad (4)$$

where, constants  $K_1$  and  $K_2$  depend on the chemical and physical properties of the polymer host and  $d_{\text{eff}}$  is the effective diameter of the penetrant. This correlation is claimed to be valid for both glassy and rubbery polymers, as well as for homopolymers and copolymers [67]. Fig. 5 shows the logarithm of the calculated diffusion coefficients of penetrants at 300 K versus their squared effective diameters. Here for argon the Lennard–Jones diameter,  $\sigma$ , is adopted as the effective diameter. Methane and propane were approximated as spherical molecules. In the case of the linear molecules, nitrogen and carbon dioxide, two extreme approximations were taken into account; adopting the spherical shape for molecules and adopting the Lennard–Jones diameter of one site as the effective diameter of molecules.

The results in Fig. 5 show that the logarithm of diffusion coefficient as a function of square effective diameter nearly follows a linear trend for spherical molecules argon, methane, and propane. Approximating the linear molecules, nitrogen and carbon dioxide, as spherical molecules leads to high deviations between the trend

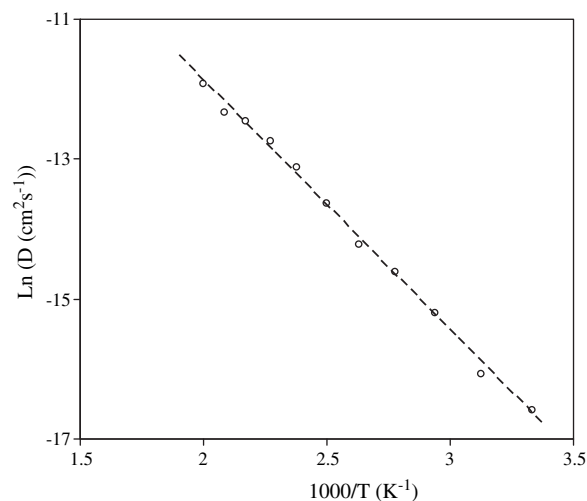


Fig. 7. Arrhenius plot of  $\ln(D)$  versus  $1/T$  for nitrogen. The dashed line indicates the best fit through the points.

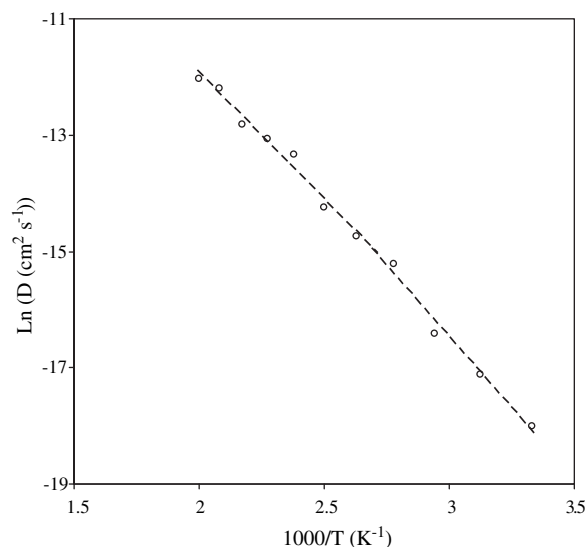


Fig. 8. Arrhenius plot of  $\ln(D)$  versus  $1/T$  for methane. The dashed line indicates the best fit through the points.

seen in the case of spherical molecules. However, the results in Fig. 5 show that adopting the Lennard–Jones of one site as the effective diameter is a better approximation for these molecules. In fact for linear molecules, an axial motion is more likely to result in a successful jump than a lateral one [17].

#### 4.3. Temperature-dependence of the diffusion coefficients

Barrer [68] was the first one who showed that the diffusion of small-size molecules in rubbery polymers is a thermally activated process. A great number of data in literature suggest that the transport coefficients (namely  $Pe$ ,  $D$ , and  $S$ ) depend on temperature, at a given pressure, via Arrhenius's law on a narrow range of temperatures [65], i.e.,

$$D = D_0 e^{-\frac{E_d}{RT}} \quad (5)$$

where  $E_d$  is the apparent activation energy,  $T$  is the temperature, and  $R$  is the gas constant. According to free volume models, at high temperatures the penetrant molecules follow a liquidlike

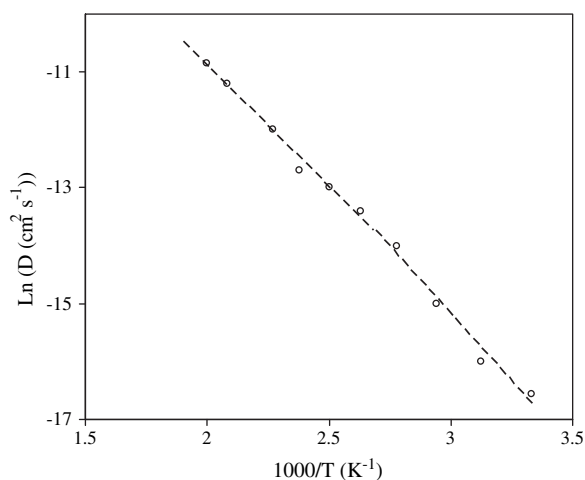
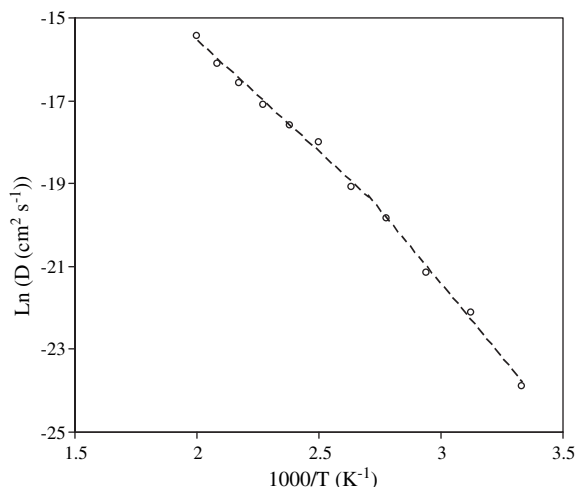


Fig. 9. Arrhenius plot of  $\ln(D)$  versus  $1/T$  for carbon dioxide. The dashed line indicates the best fit through the points.





**Fig. 10.** Arrhenius plot of  $\ln(D)$  versus  $1/T$  for propane. The dashed line indicates the best fit through the points.

mechanism and the activation energy decreases. As the temperature increases, the total free volume increases and the penetrant gas molecules can move more freely inside the amorphous materials. When the temperature is high enough the constraint of polymer chains to the movement of the diffusant molecule almost disappears and it looks like the gas molecule moves quasifreely, as in a liquid. Conversely, at low temperatures, i.e., near or below the polymer glass transition temperature, the formation or closing of above-mentioned microvoids becomes a rare event, and the activation energy increases.

According to Eq. (5), the fraction of diffusing molecules able to surmount the activation energy, ranges from 1.0 at high temperatures to 0 at very low temperatures. Arrhenius plots of  $\ln(D)$  versus  $1/T$  for afore-cited penetrant gases in host polystyrene are shown in Figs. 6–10. From the results in Figs. 6 and 7, for temperature-dependence of the diffusion coefficient of argon and nitrogen, it is seen that a linear relationship is valid between  $\ln(D)$  and  $1/T$  over the whole temperature range studied, 300–500 K. On the other hand the temperature-dependence of the diffusion coefficients of methane, carbon dioxide, and propane show a break at glass transition temperature. The temperature-dependence of the diffusion coefficient of diffusants in polymers has been the subject of a number of studies [69]. It is reported by some researchers that the Arrhenius's plot of  $\ln(D)$  as a function of  $1/T$  presented two zones separated by the glass transition and characterized by different activation energies [70,71]. At glassy state, the jump probability is small, which corresponds to higher activation energy. On the other

**Table 2**

Comparison of the calculated activation energy for diffusion of penetrants in polystyrene with experimental data [57,59,60] and with the results of former simulation works [28]. The numbers in parenthesis show the activation energies at temperatures higher than the glass transition temperature.

Penetrant	$E_d$ (kJ mol <sup>-1</sup> )	
	Experimental/simulation	This work
Ar	25.0 <sup>a</sup>	25.0
N <sub>2</sub>		30.5
CO <sub>2</sub>	44.0 <sup>b</sup>	38.6 (34.7)
CH <sub>4</sub>	36 <sup>a</sup> , 49.0 <sup>c</sup>	40.0 (35.5)
C <sub>3</sub> H <sub>8</sub>	55.0 <sup>d</sup>	59.0 (46.0)

<sup>a</sup> Ref. [57].

<sup>b</sup> Ref. [59].

<sup>c</sup> Ref. [28].

<sup>d</sup> Ref. [60].

**Table 3**

Comparison of calculated gas permeability coefficients at 300 K with experimental values [72] and with former simulation results [67].

Penetrant	$Pe \times 10^{15}$ (cm <sup>3</sup> (STP) cm/cm <sup>2</sup> Pa s)		
	Experimental	Previous simulations	This work
Ar	152	460	284
N <sub>2</sub>	45.6	180	109
CO <sub>2</sub>	988	2000	2450
CH <sub>4</sub>	60.8	130	166
C <sub>3</sub> H <sub>8</sub>			10.1

hand, at temperatures higher than the glass transition temperature the chain segmental mobility is much more important, which corresponds to lower activation energies.

The calculated activation energy in the temperature range below and above the glass transition temperature are tabulated in Table 2, and are compared with the experimental activation energies [57,59,60] and with the results obtained from former simulation studies [28]. The results for argon and carbon dioxide are quite comparable with the experimental data [57,59]. For methane our calculated activation energy is lower than the calculated value by Han and Boyd [28]. The activation energy depends on the characteristic motions of the macromolecule in a given temperature domain.

#### 4.4. Permeability coefficients

The permeabilities have been calculated employing Eq. (3), using our previously reported solubility coefficients [39] and the calculated diffusion coefficients in this work. In previous work [39], we calculated the solubilities of penetrants in polystyrene over a wide range of temperatures and pressures by performing two independent simulations, one in the polymer phase and one in the gas phase. From the simulation of the condensed phase, the excess chemical potentials are calculated using a Widom's test particle insertion method [71]. The chemical potentials were then expanded in terms of pressure employing a recent method by Vrabec and Hasse [72]. Another simulation in the grand canonical ensemble of the gas phase is shown to be sufficient to find the phase coexistence point [73,74]. Table 3 compares the calculated permeability coefficients with those of experimental values [75] and the former calculations by Kucukpinar and Doruker [67]. The results show that our calculated permeability coefficients are higher than the

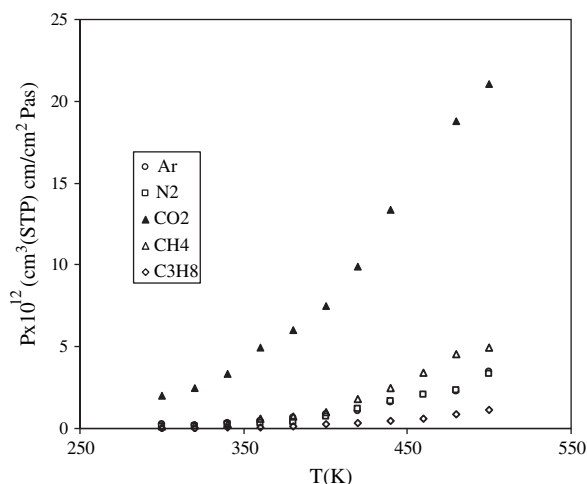


**Fig. 11.** Calculated permeability coefficients at zero pressure limit as a function of temperature.

**Table 4**

Comparison of calculated ratios of permeability coefficients at 300 K with experimental values [75] and with former simulation results [67].

Penetrant	P/P <sub>N<sub>2</sub></sub>		
	Experimental	Previous simulations	This work
N <sub>2</sub>	1.0	1.0	1.0
Ar	3.33	2.55	2.6
CO <sub>2</sub>	21.66	11.11	22.47
CH <sub>4</sub>	1.33	0.72	1.52
C <sub>3</sub> H <sub>8</sub>			0.093

experimental values [75], as a result of overestimating the solubility coefficients in computer simulation methods [39]. The same trend is seen in the calculated permeability coefficients by Kucukpinar and Doruker [67]. The calculated permeability coefficients over a temperature range of 300–500 K are also shown in Fig. 11. The results in Fig. 11 show that polystyrene is much permeable to CO<sub>2</sub>, compared to other gases studied in this work, because of the higher solubility coefficient of CO<sub>2</sub> in polystyrene and its relatively higher diffusion coefficient. On the other, polystyrene is less permeable to the biggest penetrant molecule, propane, because of its very small diffusion coefficient.

We have also compared our calculated permeability coefficient ratios (selectivities) in the zero pressure limit with the corresponding experimental values [75] and the calculations by Kucukpinar and Doruker [67]. In Table 4, we have listed the ratios of permeability coefficients at 300 K to that of nitrogen's permeability and compared the results with experimental measurements [75] and with the former calculations by Kucukpinar and Doruker [67]. The results in Table 4 show that the calculated ratios are quite close to the experimental ratios and are in a much better agreement with experiment [75] compared to the calculations by Kucukpinar and Doruker [67]. One reason for this is the fact that Kucukpinar and Doruker [67] have used united-atom models for both polymer and diffusant gases, while more detailed atomistic force fields have been used in this work. This shows that our calculated permeability coefficients are higher than the experimental values by nearly the same factor. The same conclusion was made in our former work on the calculated solubility coefficients [39].

## 5. Conclusions

The diffusion coefficients of penetrant gases in polystyrene have been calculated over a wide range of temperatures, 300 K–500 K. The calculated diffusion coefficients agree well with the experimental data [57–60] and with former simulation results [28,61]. The jumping mechanism of penetrant gases in polystyrene is confirmed. Our results show that the diffusion regime begins in a shorter time at higher temperatures, and fluctuations in the center-of-mass mean-square displacements depend on the penetrant size. The logarithm of the diffusion coefficient appears to vary linearly with the square effective diameter of the penetrant molecule, supporting the validity of the correlation scheme by Teplyakov and Meares [66]. The calculated permeability coefficients are higher than the experimental data [75], but they are in agreement with former simulation studies [67]. This is due to the fact that computer simulation studies overestimate the solubility coefficients [39]. The ratios of permeability coefficients (selectivities) calculated in this work are in a very good agreement with experimental data [75] and follow the same trend observed in our calculated solubility coefficients [39].

From the results of our calculations at temperature regimes below and above the glass transition temperature, it is concluded that for gases like argon and nitrogen, the Arrhenius plot of  $\ln(D)$

versus  $1/T$  is almost linear over the whole temperature range. But for some gases like carbon dioxide, methane, and propane the results show that two different slopes do exist for the Arrhenius plot, below and above the glass transition temperature. While the results of Han and Boyd [28] on the calculated diffusion coefficient of methane in polystyrene does not show the slope change at glass transition temperature, our results are in agreement with experimental findings [70,71].

## References

- [1] Vrentas JS, Duda JL. *J Polym Sci Polym Phys* 1977;15:403.
- [2] Vrentas JS, Duda JL. *J Polym Sci Polym Phys* 1977;15:417.
- [3] Vrentas JS, Duda JL. *AIChE J* 1979;25:1.
- [4] Vrentas JS, Duda JL, editors. *Diffusion. Encyclopedia of polymer science and engineering*, vol. 5. New York: Wiley; 1986. p. 36–68.
- [5] Mauritz KA, Storey RF, George SE. *Macromolecules* 1990;23:441.
- [6] Mauritz KA, Storey RF. *Macromolecules* 1990;23:2033.
- [7] Ganesh K, Nagarajan R, Duda JL. *Ind Eng Chem Res* 1992;31:746.
- [8] Arizzi S. *Diffusion of small molecules in polymeric glasses: a modelling approach*. Ph.D. Thesis, Massachusetts Institute of Technology, Boston; 1990.
- [9] Gusev AA, Arizzi S, Suter UW. *J Chem Phys* 1993;99:2221.
- [10] Gusev AA, Suter UW. *J Chem Phys* 1993;99:2228.
- [11] Gusev AA, Müller-Plathe F, van Gunsteren WF, Suter UW. *Adv Polym Sci* 1994;116:207.
- [12] Greenfield ML, Theodorou DN. *Macromolecules* 1993;26:5461.
- [13] Greenfield ML, Theodorou DN. *Polym Prepr (Am Chem Soc)* 1995;36:687.
- [14] Gray-Weale AA, Henchman RH, Gilbert RG, Greenfield ML, Theodorou DN. *Macromolecules* 1997;30:7296.
- [15] Karayiannis NCh, Mavrantzas VG, Theodorou DN. *Macromolecules* 2004;37:2978.
- [16] Müller-Plathe F. *J Chem Phys* 1991;94:3192.
- [17] Müller-Plathe F. *J Chem Phys* 1992;96:3200.
- [18] Müller-Plathe F. *Acta Polym* 1994;45:259.
- [19] Milano G, Guerra G, Müller-Plathe F. *Chem Mater* 2002;14:2977.
- [20] Boyd RH, Pant PVK. *Macromolecules* 1991;24:6325.
- [21] Müller-Plathe F, Rogers SC, van Gunsteren WF. *Chem Phys Lett* 1992;199:237.
- [22] Sok RM, Berendsen HJC, van Gunsteren WF. *J Chem Phys* 1992;96:4692.
- [23] Müller-Plathe F, Rogers SC, van Gunsteren WF. *Macromolecules* 1992;25:6722.
- [24] Pant PVK, Boyd RH. *Macromolecules* 1993;26:679.
- [25] Gee RH, Boyd RH. *Polymer* 1995;36:1435.
- [26] Smit E, Mulder MHV, Smolders CA, Karrenbeld H, Eerden J, Feil D. *J Memb Sci* 1992;73:247.
- [27] Zhang R, Mattice WL. *J Memb Sci* 1995;108:15.
- [28] Han J, Boyd RH. *Polymer* 1996;37:1797.
- [29] Hofman D, Ulbrich L, Fritsch D, Paul D. *Polymer* 1996;37:4773.
- [30] Freid JR, Goyal D. *J Polym Sci Polym Phys* 1998;35:519.
- [31] Lim SY, Tsotsis TT, Sahimi M. *J Chem Phys* 2003;119:496.
- [32] Müller-Plathe F. *Macromolecules* 1991;24:6475.
- [33] Tamai Y, Tanaka H, Nakanishi K. *Macromolecules* 1995;28:2544.
- [34] Pricl S, Fermeglia M. *Chem Eng Commun* 2003;190:1267.
- [35] Abu-Shargh BF. *Polymer* 2004;45:6383.
- [36] Cuthbert TR, Wagner NJ, Paulaitis ME. *Macromolecules* 1990;23:5017.
- [37] Mooney DA, MacElroy JMD. *J Chem Phys* 1999;110:11087.
- [38] Cuthbert TR, Wagner NJ, Paulaitis ME. *Macromolecules* 1997;30:3058.
- [39] Eslami H, Müller-Plathe F. *Macromolecules* 2007;40:6413.
- [40] Eslami H, Müller-Plathe F. *J Comput Chem* 2007;28:1763.
- [41] Haus JW, Kehr KW. *Phys Rep* 1987;150:265.
- [42] Baumgärtner A, Moon M. *Europhys Lett* 1989;9:203.
- [43] Gusev AA, Suter UW, Moll DJ. *Macromolecules* 1995;28:2582.
- [44] Gusev AA, Suter UW. *Phys Rev A* 1991;43:6488.
- [45] Tamai Y, Tanaka H, Nakanishi K. *Macromolecules* 1994;27:4498.
- [46] Müller-Plathe F, Rogers SC, van Gunsteren WF. *J Chem Phys* 1993;98:9895.
- [47] Müller-Plathe F. *Macromolecules* 1996;29:4782.
- [48] Müller-Plathe F. *J Chem Phys* 1995;103:4346.
- [49] Jorgensen WL, Severance DL. *J Am Chem Soc* 1990;112:4768.
- [50] Allen MP, Tildesley DJ. *Computer simulation of liquids*. Oxford: Clarendon Press; 1987.
- [51] Rapold RF. Ph.D. Thesis, Swiss Federal Institute of Technology Zürich; 1993.
- [52] Berendsen HJC, Postma JPM, van Gunsteren WF, DiNola A, Haak JR. *J Chem Phys* 1984;81:3684.
- [53] Ryckaert JP, Ciccotti G, Berendsen HJC. *J Comput Phys* 1997;23:327–41.
- [54] Müller-Plathe F, Brown D. *Comput Phys Commun* 1991;64:7–14.
- [55] Müller-Plathe F. *Comput Phys Commun* 1993;78:77–94.
- [56] Müller-Plathe F, Laaksonen L, van Gunsteren WF. *J Mol Graph* 1993;11:118–20.
- [57] Rein DH, Badour RF, Cohen RE. *J Appl Polym Sci* 1992;45:1223–7.
- [58] Van Krevelen DW. *Properties of polymers*. Netherlands: Elsevier Science; 1990 [Chapter 18].
- [59] Crank J, Park GS, editors. *Diffusion in polymers*. 2nd ed. New York: Academic Press; 1975.

- [60] Barrie JA, Williams MJL, Munday K. *Polym Eng Sci* 1980;20:20.
- [61] Stannett VT. In: Crank J, Park GS, editors. *Diffusion in polymers*. London: Academic; 1968. p. 41.
- [62] Kumins CA, Kwei TK. In: Crank J, Park GS, editors. *Diffusion in polymers*. London: Academic; 1968. p. 107.
- [63] Raucher D, Sefcik MD. *ACS Symp Ser* 1983;223:111.
- [64] Rogers CE. In: Comyn J, editor. *Polymer permeability*. London: Elsevier; 1985.
- [65] Griskey RG. *AIChE Symp Ser* 1977;73:158.
- [66] Teplyakov V, Meares P. *Gas Sep Purific* 1990;4:66.
- [67] Kucukpinar E, Doruker P. *Polymer* 2003;44:3607.
- [68] Barrer RM. *Nature* 1937;140:106.
- [69] Klopffer MH, Flaconnèche B. *Oil Gas Sci Tech* 2001;56:223.
- [70] Michaels AS, Vieth WR, Barrie JA. *J Appl Phys* 1963;34:13.
- [71] Meares P. *J Am Chem Soc* 1954;76:3415.
- [72] Widom B. *J Chem Phys* 1963;39:2808.
- [73] Vrabc J, Hasse H. *Mol Phys* 2002;100:3375.
- [74] Eslami H, Dargahi A, Behnejad H. *Chem Phys Lett* 2009;473:66.
- [75] Csernica J, Baddour RF, Cohen RE. *Macromolecules* 1987;20:2468.